Pramāṇa, Vol. 18, No. 3, March 1982, pp. 279–289. © Printed in India.

Coherent pion-photoproduction by deuterons at intermediate energies

V S BHASIN, V K GUPTA and J D ANAND
Department of Physics, University of Delhi, Delhi 110 007, India

Abstract. Non-relativistically exact single scattering calculations for coherent pion photoproduction by deuterons at intermediate photon energies (200 MeV to 500 MeV) are presented. For the two-body $\gamma N \to \pi N$ process we use the well-known dispersion theoretic model by Chew *et al* and for the deuteron wave-functions we employ the Yamaguchi and the two term Gaussian wave-function. We find that while both the wavefunctions reproduce the deuteron e.m. form factor reasonably well, the results for the pion photoproduction cross-section show, however, a sensitive dependence on their detailed forms. The angular distributions at various energies are found to have considerable variations from the usual impulse approximation calculations but tend to improve the agreement with the data in a large kinematical region.

Keywords. Nuclear reactions; single scattering; impulse approximation; pion photoproduction; deuteron wavefunction.

1. Introduction

In the recent past there has been a renewed interest (Laget 1981; Argan *et al* 1979; Booth *et al* 1979) in the experimental as well as theoretical studies of photopion production processes both in the resonance region and near threshold energies using light nuclear targets such as deuterons and tritons. Thus, in a series of papers Laget and his coworkers (Laget 1978) studied the various photopion production processes by deuterons starting from a rather simple model where the pion photoproduction on nucleon is described by the Born terms and the s-channel (3, 3) resonance. While for $\gamma d \to \pi^- pp$ they employ the spectator model and investigate within this framework, the rescattering effects, for coherent neutral pion photoproduction on deuterons they compute the Feynman diagrams in the non-relativistic limit to estimate the effect of Fermi motion and the rescattering corrections.

In more recent calculations on photopion production processes (Anand *et al* 1980; Gupta *et al* 1980), we have employed the well-known dispersion theoretic model by Chew *et al* (Chew *et al* 1957; Nishijima 1965) (commonly referred to as CGLN) for $\gamma N \to \pi N$ amplitude wherein not only the pole terms but the full pion-nucleon continuum manifestly appears through partial wave amplitudes. In the first paper (Anand *et al* 1980) the main thrust was to study, in $\gamma d \to \pi^- pp$ at medium energies the sensitiveness of off-energy-shell effects of the $\gamma N \to \pi N$ amplitude and to investigate the role of the deuteron wave-functions used. The second (Gupta *et al* 1980) was devoted towards analysing the role of n-n final state interaction in $\gamma d \to \pi^+ nn$ near threshold energies.

The present paper is in direct continuation of the earlier two referred above. Here we study the coherent photopion production by deuterons at medium energies by calculating exactly the single scattering amplitude in a non-relativistic approach. The essential ingredients are (i) the CGLN model for the two-body $\gamma N \to \pi N$ process, and (ii) the Yamaguchi (1954) and the two term Gaussian deuteron wave-function. The objective is two-fold: (i) to show the effect of Fermi motion and off-energy-shell contribution by comparing the exact single scattering results with the usual impulse approximation, and (ii) to point out the sensitiveness of the results on the detailed structure of the deuteron wave-functions used. In addition, the analysis also brings out the sensitive role played by kinematical factors of the two-body subprocess $\gamma N \to \pi N$ used in different reference frames.

In §2 we outline the necessary steps to write down the expressions for T-matrix and differential cross-section for the process $\gamma d \to \pi^\circ d$. As the two-body input amplitude $\gamma N \to \pi N$ has already been described in I, we shall only be brief here and refer, whereever necessary, to I for details. In § 3 we give the results and discuss the various features of the present analysis.

2. Formalism

The T-matrix for the process $\gamma d \to \pi^\circ d$ is written down explicitly (figure 1) as

$$\langle {}^3\chi_{1m'} \mid T(\mathbf{k}_\pi, \mathbf{k}_i, \hat{\epsilon}; W) \mid {}^3\chi_{1m} \rangle = \langle {}^3\chi_{1m'} \mid \int d\mathbf{p}\, \phi_d(\mathbf{p} - \mathbf{k}_\pi/2) \times t(\mathbf{k}'_\pi, \mathbf{k}'_i, \hat{\epsilon}'; W')\, \phi_d(\mathbf{p} - \mathbf{k}_i/2) \mid {}^3\chi_{1m} \rangle, \tag{1}$$

where ϕ_d is the deuteron wave-function, ${}^3\chi_{1m}$ is its spin state, $\mathbf{k}_i$ and $\mathbf{k}_\pi$ are respectively the incoming photon and the outgoing pion momenta in γ-d c.m. system; W is the c.m. energy:

$$W = k_i + (k_i^2 + M_d^2)^{1/2}. \tag{2}$$

The $t(\mathbf{k}'_\pi, \mathbf{k}'_i, \hat{\epsilon}'; W')$ in (1) represents the off-energy-shell T-matrix for the subprocess $\gamma N \to \pi N$; $\mathbf{k}'_\pi$, $\mathbf{k}'_i$ are the pion and photon momenta in the γ-N c.m. system and W' is the c.m. energy

$$W' = k'_i + (k'^2_i + m^2)^{1/2}. \tag{3}$$

The momenta $\mathbf{k}'_i$, and $\mathbf{k}'_\pi$ are related to the corresponding momenta $\mathbf{k}_i$ and $\mathbf{k}_\pi$ in

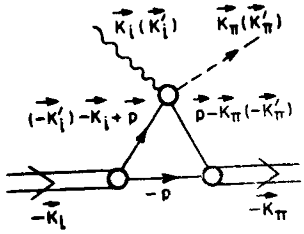

Figure 1. Single scattering diagram for the process $\gamma d \to \pi^\circ d$. The momenta in the parentheses refer to the values in γN c.m. system.

the γ-d c.m. system in a non-relativistic limit (when the internal momentum $\mathbf{p}$ is taken to be small) *viz:*

$$\mathbf{k}_t' = \mathbf{k}_t - k_t\,\mathbf{p}/(k_t + m);\ \mathbf{k}_\pi' = \mathbf{k}_\pi - k_\pi^0\,\mathbf{p}/(k_t + m), \tag{4}$$

in which case the polarization vector of the photon in both the systems is the same (*i.e.* $\hat{\epsilon}' = \hat{\epsilon}$).

To generalize the T-matrix incorporating spin, i-spin structure for the $\gamma N \to \pi N$ amplitude, we follow the notations outlined in I. We note here that for π° photoproduction on proton or neutron in the deuteron, we have only

$$t_{\gamma N \to \pi^\circ N} = f^{(+)} + f^{(0)}\,\tau_3 \tag{5}$$

However, the expectation value of τ_3 for iso-singlet deuteron being zero, it is the $f^{(+)}$ component which eventually survives. As for the spin structure we have (equation (2.12) in I.)

$$f^{(+)} = a^{(+)} + i\boldsymbol{\sigma}\cdot\mathbf{b}^{(+)}, \tag{6}$$

where $a^{(+)}$ and $\mathbf{b}^{(+)}$ are explicitly given in the appendix in I. Before we feed the structure of $a^{(+)}$ and $\mathbf{b}^{(+)}$ in the integral (1) we need a transformation of the integration variable vector $\mathbf{p}$ to $\mathbf{k}_\pi'$. This is essentially to avoid the unnecessary complications arising due to the fact that $a^{(+)}$ and $\mathbf{b}^{(+)}$ involve π-N p-wave amplitudes in terms of the phase-shifts. These phase-shifts, being the function of k_π' would then involve, by (4), not only the magnitudes of $\mathbf{k}_\pi$ and $\mathbf{p}$ but the angle between them also. By using second of the equations in (4) which implies

$$\mathbf{p} \to C\,(\mathbf{k}_\pi - \mathbf{k}_\pi'), \tag{7}$$

where

$$C = (k_t + m)/k_\pi^0$$

we rewrite the T-matrix (1) as

$$\begin{aligned}\langle {}^3\chi_{1m'}|\,T\,(\mathbf{k}_\pi, \mathbf{k}_t\,\hat{\epsilon};\,W)\,|\,{}^3\chi_{1m}\rangle = \langle {}^3\chi_{1m'}|\,C^3 \textstyle\int \mathrm{d}\,\mathbf{k}_\pi'\,\phi_d((C-\tfrac{1}{2})\,\mathbf{k}_\pi - C\mathbf{k}_\pi')\\ [a^+(\mathbf{k}_\pi', \mathbf{k}_t', \hat{\epsilon};\,W') + i\,\boldsymbol{\sigma}\cdot\mathbf{b}^{(+)}(\mathbf{k}_\pi', \mathbf{k}_t', \hat{\epsilon};\,W')]\\ \times\,\phi_d\,(C\,\mathbf{k}_\pi - \mathbf{k}_t/2 - C\,\mathbf{k}_\pi')\,|\,{}^3\chi_{1m}\rangle,\end{aligned} \tag{8}$$

where

$$\mathbf{k}_t' = \mathbf{k}_t - k_t\,(\mathbf{k}_\pi - \mathbf{k}_\pi')/k_\pi^0, \tag{9}$$

We now substitute the expressions for $a^{(+)}$ and $\mathbf{b}^{(+)}$ (given in I) and observe that we can read, on general grounds, the structure of the T-matrix from (8) quite independently of the detailed nature of the deuteron wave-functions used. Thus,

$$\langle {}^3\chi_{1m'} | T(\mathbf{k}_\pi, \mathbf{k}_i\, \hat{\epsilon}; W) | {}^3\chi_{1m} \rangle = \langle {}^3\chi_{1m'} | \hat{\epsilon}\cdot(\mathbf{k}_\pi \times \mathbf{k}_i)\, a_1 + i\,\sigma\cdot[\hat{\epsilon}\, a_2 + \mathbf{k}_i\,(\hat{\epsilon}.\, \mathbf{k}_\pi)\, a_3 + \mathbf{k}_\pi\,(\hat{\epsilon}\cdot\mathbf{k}_\pi)\, a_4] | {}^3\chi_{1m} \rangle, \tag{10}$$

where a_1, a_2, a_3 and a_4 are the complex scalar functions involving the overlap integrals with deuteron wave-functions and the π-N amplitudes. Indeed, to evaluate these integrals one requires the detailed knowledge of the deuteron wave-functions. A similar structure for the T-matrix in terms of a's involving rather complicated integrals can also be obtained if one includes the tensor component of the deuteron. However, we at present restrict our investigation only to the s-state deuteron wave-function. The square of the matrix-element (10) after summing over the final and averaging over the initial spin states of the deuteron is worked out to be

$$1/3\ \mathrm{Tr}\ (T^+T) = (4/3)\ [k_i^2\, k_\pi^2 \sin^2\theta\ (3\,|a_1|^2/2 + |a_3|^2) + 2\,|a_2|^2 + k_\pi^2 \sin^2\theta\ (k_\pi^2\ |a_4|^2 + 2\ \mathrm{Re}\ (a_2^*\, a_4) + 2\ (\mathbf{k}_i\cdot\mathbf{k}_\pi)\ \mathrm{Re}\ (a_3^*\, a_4))], \tag{11}$$

which is related to the differential cross-section

$$\mathrm{d}\sigma = \frac{E_\pi\, E_{d'}\, E_\gamma\, E_d}{(2\pi)^2\, W^2}\, \frac{k_\pi}{k_i}\, \frac{1}{3}\, \mathrm{Tr}\ (T^+\, T) \tag{12}$$

In (12) E_π, E_d' denote respectively the final pion and the deuteron energies while E_γ, E_d, those of the initial photon and deuteron — all in γ-d c.m. system and θ in (11) is the γ-d c.m. angle.

We recall that for $\gamma N \to \pi N$ t-matrix we have a relation similar to (12); *viz.*

$$\mathrm{d}\sigma_{\gamma N\to\pi N} = \frac{E_\gamma'\, E_N'\, E_\pi'\, E_{N'}'}{(2\pi)^2\, W'^2}\, \frac{k_\pi'}{k_i'}\, |t|^2, \tag{13}$$

while a more familiar relation is

$$\mathrm{d}\sigma_{\gamma N\to\pi N} = \frac{k_\pi'}{k_i'}\, |f|^2, \tag{14}$$

in terms of which the CGLN amplitudes are, in fact, given. We thus require a transformation

$$t \to \frac{2\pi\, W'}{[E_\gamma'\, E_N'\, E_\pi'\, E_{N'}']^{1/2}}\, f, \tag{15}$$

where E_γ', E_N', E_π', $E_{N'}'$ represent respectively the energies of the photon, initial nucleon, pion and the final nucleon in the γ-N c.m. system. The photon momentum,

$\mathbf{k}_{i}'$ as given by (9) is quite complicated involving various angles with the integration vector $\mathbf{k}_{\pi}'$.

We circumvent this difficulty by determining k_{i}' through energy conservation in γ-N c.m. frame. Thus, knowing E_{π}' and $E_{N'}'$ in terms of k_{π}' - the pion momentum (which is the variable of integration), we have

$$W' = E_{\pi}' + E_{N'}$$

$$= E_{\gamma}' + E_{N}' = k_{i}' + (k_{i}'^{2} + m^{2})^{1/2},$$

so that

$$k_{i}' = (W'^{2} - m^{2})/2\, W'.$$

Here, indeed all the kinematical energy factors of the sub-two-body process, being the function of k_{π}', will be appearing inside the integral. In addition to employing this choice (referred to as γNC) we have also made an alternative rather simplified choice of assuming $\mathbf{k}_{i}' = \mathbf{k}_{i}$ (and $\mathbf{k}_{\pi}' = \mathbf{k}_{\pi}$) *i.e.* determining the two-body kinematics in the γ-d c.m. system. This is adopted in the same spirit as used in impulse approximation where one has an on-shell two body amplitude whose kinematics are generally determined from the main process. Obviously in this choice (referred to as γd frame), all the kinematical factors will factor out of the integral.

We also record here, for completeness, the expression for the T-matrix in the impulse approximation, *viz.*

$$T = S(q/2)\, t(\mathbf{k}_{\pi}, \mathbf{k}_{i}, \hat{\epsilon}; W), \tag{16}$$

where

$$S(q/2) = \int d\mathbf{p}\, \phi_{d}(\mathbf{p} - \mathbf{k}_{\pi}/2)\, \phi_{d}(\mathbf{p} - \mathbf{k}_{i}/2),$$

is the deuteron form-factor, and

$$\mathbf{q} = \mathbf{k}_{\pi} - \mathbf{k}_{i},$$

is the momentum transfer between the initial photon and the final pion.

As for the deuteron wave-functions, we employ, (i) the well-known Yamaguchi wave function [Yamaguchi 1954]

$$\phi_{d}(p) = Ng(p)/(p^{2} + \alpha^{2}), \quad g(p) = 1/(p^{2} + \beta^{2});$$

N is the deuteron normalization, $\beta = 1{\cdot}449\ \mathrm{fm}^{-1}$ and $\alpha = 0{\cdot}2316\ \mathrm{fm}^{-1}$; and (ii) the two term Gaussian wavefunction

$$\phi_{d}(p) = a \exp(-\alpha p^{2}) + b \exp(-\beta p^{2}).$$

The various constants are

$$a = 2{\cdot}211\ \mathrm{fm}^{3/2}, \qquad b = 0{\cdot}2934\ \mathrm{fm}^{3/2},$$

$$\alpha = 6{\cdot}123\ \mathrm{fm}^{2}, \qquad \beta = 0{\cdot}8264\ \mathrm{fm}^{2}.$$

Clearly the two terms in the Gaussian are required to describe the short and the long range part of the wave-function. Both these wavefunctions are realistic enough so as to reproduce the deuteron form-factor in reasonable agreement with the experimental data. In particular, the two-term Gaussian wave function does a rather good job while the Yamaguchi wave-function still has room for including the tensor and the soft core repulsive terms. It is worth pointing out, however, that our main objective here is not so much to employ the ' best ' wavefunction as to illustrate the sensitiveness of the results on the nature of the wavefunction used.

3. Results and discussion

In figure 2 is depicted the differential cross-section at $\theta_{c.m.} = 90°$ versus photon lab. energy. Curiously enough the Yamaguchi wave-function predicts the results using γN kinematics in γ-d frame in remarkably good agreement with experimental data (Von Hotley *et al* 1973), while the Gaussian wave-function yields results 50-60% higher. Even the Yamaguchi wave-function with kinematical energy factors

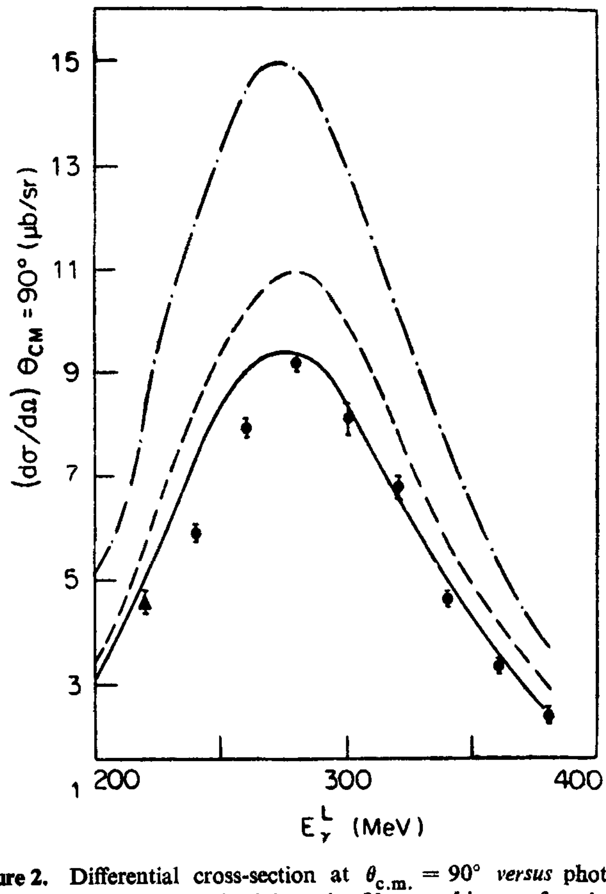

Figure 2. Differential cross-section at $\theta_{c.m.} = 90°$ *versus* photon lab. energy E_γ^L (MeV). Full line is obtained by using Yamaguchi wave-function for the deuteron and γN kinematics in γd frame; dashed line is when γN kinematics are taken in γ-NC frame and the dot-dashed line is by using two term Gaussian wave-function and γN amplitude in γd frame. The data points are from Von Hotley *et al* (1973).

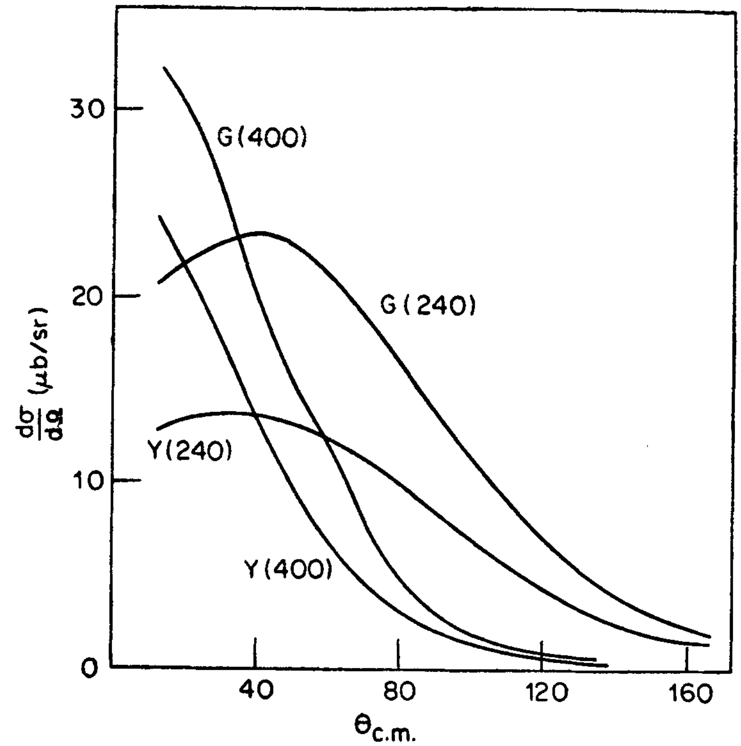

Figure 3. Comparison of results for the differential cross-section *versus* $\theta_{c.m.}$ between Yamaguchi (Y) and the two term Gaussian (G) wave functions using γN amplitude in γNC frame. The figures in the parantheses refer to photon lab. energy.

for γN amplitude taken in γNC frame, contributes about 15% more. To show a detailed difference in behaviour for the wave-functions, we have plotted in figure 3 the differential cross-section *versus* $\theta_{c.m.}$ for photon lab. energies at 240 MeV and 400 MeV. The behaviour at the other energies *viz.* 280 MeV and 360 MeV is similar in nature to 240 MeV and 400 MeV respectively and has therefore not been shown in the figure. At large angles ($\theta_{c.m.} \gtrsim 100°$) and for almost all the energies the difference in the results is narrowed down. This could possibly be due to the fact that large momentum components of the deuteron wave-function are not as sensitive. However, the difference for smaller energies and at smaller angles ($\theta_{c.m.} \sim 90°$) is rather marked indicating thereby a significant role played by the small momentum components of the wave-functions used. Apparently, the large area swept by the wave-function along with $\gamma N \rightarrow \pi N$ amplitude for small values of the integration variable k'_π as well as of k_t and k_π is quite sensitive to the nature of the wave-function. Our earlier experience (page 2014 of I) with Yamaguchi and Gaussian wave-functions shows that while for smaller values of the internal momenta ($\sim$ 70 MeV/c) of the deuteron, Yamaguchi is slightly larger in magnitude than Gaussian but then it has a sharper fall so that for momenta lying between 70 MeV/c to $\sim$ 210 MeV/c, Gaussian wave-function is larger. Again for asymptotic values of the momenta, Yamaguchi dominates over the Gaussian. Now, if the major contribution of the integral is from the region corresponding to the internal deuteron momenta between 70 MeV/c to 210 MeV/c where the γN amplitude is presumably significant too, this would then

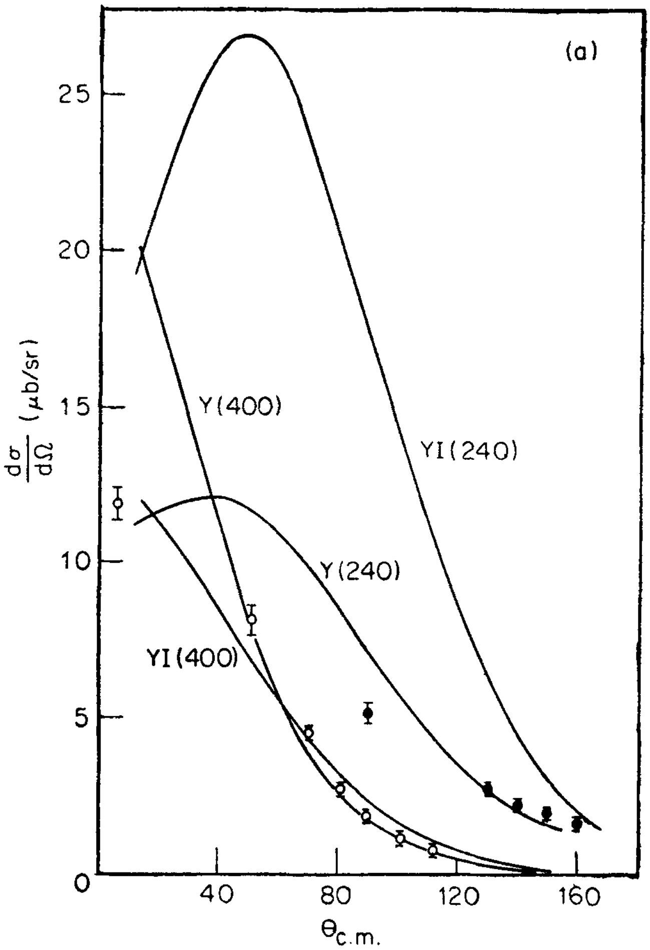

Figure 4(a).

explain why Gaussian is contributing appreciably higher than the Yamaguchi wave-function. The main point here is that it is not the deuteron form factor which determines, as is the case in impulse approximation, a quantitative trend of single scattering cross-section. On the other hand, the detailed behaviour of the wave-function, which is hardly checked independently, plays a sensitive role.

To compare the results of exact single scattering calculations with the impulse approximation and with the experimental data (Von Hotley *et al* 1973; Bonquet *et al* 1974; Hilger *et al* 1975) we plot in figures 4(a) and (b) the differential cross-section for photon lab. energies 240, 280, 360, and 400 MeV. We employ the Yamaguchi wave-function and use the kinematics of γN in γd frame so as to make a direct comparison with the results obtained in the impulse approximation. Thus for lower energies *viz.* 240 and 280 MeV, while the exact single scattering cross-section is considerably reduced at all angles, at higher energies it gets enhanced near the forward direction and then decreases at larger angles—a trend which brings the results closer to experimental data as compared to impulse approximation. At higher energies $\sim$ 400 MeV and in the forward direction, the impulse approximation still appears delivering goods in terms of agreement with experiment, while at larger angles it

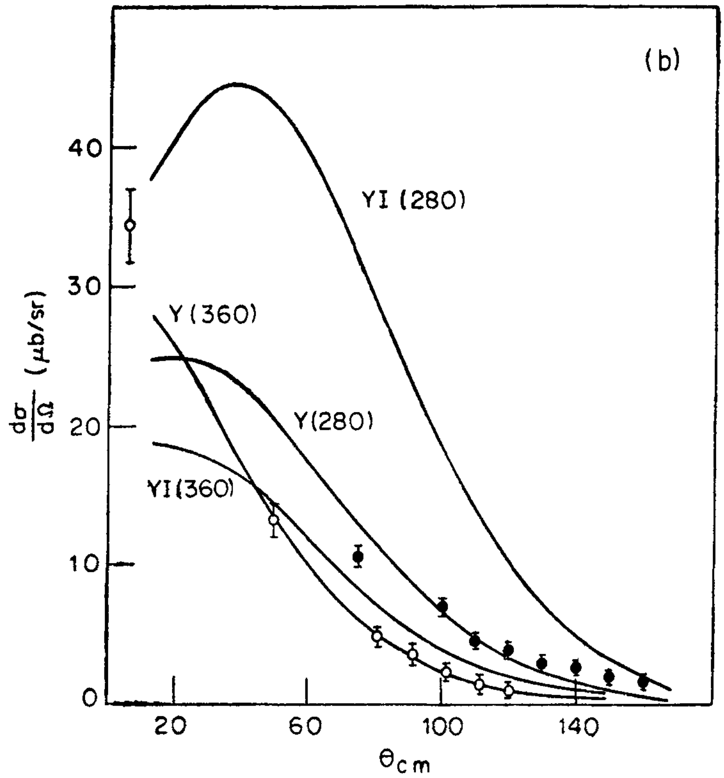

Figure 4(b).

Figures 4(a) and (b). Exact single scattering results (Y) for differential cross-section *versus* $\theta_{c.m.}$ compared with impulse approximation (YI) using Yamaguchi wave-function and γ-N amplitude in γ-d frame. The solid points refer to 240 MeV and 280 MeV whereas the open circle represent the data at 360 MeV and 400 MeV. The figures in the parantheses denote the photon lab. energy.

goes off by ~15 to 20%. As for the effect of inserting γN amplitude using two-body kinematical energy factors in the two reference frames, defined earlier, we find that while γNC frame increases the cross-section by 20-25% near the forward direction, at larger angles it increases by 15-20% in the energy range considered. While the effect of these energy factors appears to be significant, it is heartening to note that the exact single scattering calculations show a marked improvement over the impulse approximation results. In particular, when the kinematics for the sub-two-body process is chosen in the γd frame, there is a remarkably good agreement with the data over the whole angular range. This is especially reassuring in view of the fact that the previous studies (Laget 1978; Osland 1976) with realistic deuteron wave-function and taking rescattering effects into account, attribute only a marginal improvement in the results.

We also find that the present calculations are in good agreement with those obtained, for instance, by Bosted and Laget (1978) using Reid soft-core wave-function for deuteron. At higher energies, *viz.* around 400 MeV, and near the forward direction, however, the calculations appear to have some variations: while our calculations show a wide departure from the impulse approximation, Laget's (1978) agree rather closely. This could possibly be due to the off-energy-shell effect of the different input $\gamma N \rightarrow \pi N$ amplitude.

In figure 5 we plot the total cross-section *versus* photon lab. energies varying from 200 MeV to $\sim$ 420 MeV, showing the effect of the deuteron wave-functions in the exact calculations and comparing with the corresponding impulse approximation results. Here again the calculations show a marked effect of the single scattering results from those obtained in impulse approximation especially near the resonance region. While the deviations in the impulse approximation calculations with the two wave-functions directly reflect the corresponding behaviour in the form factors, the single scattering cross-section, on the other hand, bears out the sensitive role played by the details of the wave-functions. To our knowledge there is no experimental data available for the total cross-section to compare with the present calculations. If the agreement obtained for differential cross-section is any indication, it is not difficult to conjecture that here again the results with the Yamaguchi wave-function should be closer to experimental data.

In conclusions, the main findings of the present analysis are:

(a) the results in exact single scattering calculations in $\gamma d \to \pi^{\circ} d$ at medium energies differ considerably from the usual impulse approximation calculations and tend to improve the agreement with the data;
(b) it is not simply the deuteron form factor but rather the details of the deuteron wave-functions which are found to play a significant role;
(c) the choice of the kinematical energy factors for the sub-two-body $\gamma N \to \pi N$ process appears to be quite sensitive.

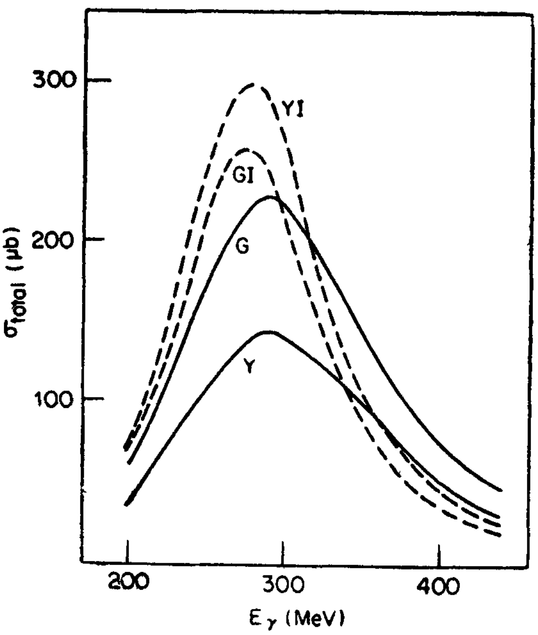

Figure 5. Total cross-section *versus* photon lab. energy with Yamaguchi (Y) and Gaussian (G) wave-functions taking the γN amplitude in γd frame. YI and GI represent the results in impulse approximation.

Indeed, the present calculations have room for refinements such as including tensor force and repulsive soft core terms in the deuteron wave-function. It is also not clear how sensitive role the off-energy-shell effects of the two-body amplitude in the CGLN model have in comparison to the one used, for instance, by Laget (1978). In addition, it should also be interesting to study, within this framework, the re-scattering effects especially near threshold energies. It is to such and the related problems that we shall be addressing ourselves in our future investigations.

References

Anand J D, Bhasin V S and Gupta V K 1980 *Phys. Rev.* **C21** 2010 (referred to as I)
Argan P *et al* 1979 *Phys. Rev.* **C20** 242
Booth E C *et al* 1979 *Phys. Rev.* **C20** 1217
Bosted P and Laget J H 1978 *Nucl. Phys.* **A296** 413
Bouquet B *et al* 1974 *Nucl. Phys.* **B79** 45
Chew G F *et al* 1957 *Phys. Rev.* **106** 1345
Gupta V K, Anand J D and Bhasin V S 1980 *Phys. Rev.* **C22** 721
Hilger E *et al* 1975 *Nucl. Phys.* **B93** 7
Laget J M 1978 *Nucl. Phys.* **A296** 388
Laget J M 1981 *Phys. Rep.* **69** 1
Nishijima K 1965 *Fundam. Part.* p. 184
Osland P and Rej A K 1976 *Nuovo Cimento* **32** 369
Von Hotley G *et al* 1973 *Z. Phys.* **259** 51
Yamaguchi Y 1954 *Phys. Rev.* **95** 1628